Temperature dependence of exchange stiffness in an off-stoichiometric Ni_2MnIn Heusler alloy

K. Niitsu,[1,2,*] X. Xu,[3] R. Y. Umetsu,[4] R. Kainuma,[3] and K. Harada[2]

[1]*Department of Materials Science & Engineering, Kyoto University, Sakyo-ku, Kyoto 606–8501, Japan*

[2]*RIKEN, Center for Emergent Matter Science (CEMS), Wako 351-0198, Japan*

[3]*Department of Materials Science, Graduate School of Engineering, Tohoku University, Sendai, 980–8579, Japan*

[4]*Institute for Materials Research, Tohoku University, Sendai, 980–8577, Japan*

(Received 8 November 2019; revised manuscript received 13 January 2020; published 29 January 2020)

Ferromagnetic exchange stiffness is a key to describe the robustness of a ferromagnetic interaction. Because the experimental determination of the exchange stiffness constant A continues to be elusive, especially at elevated temperatures, micromagnetic insights on the impact of thermal fluctuations on the ferromagnetic spin order have remained less tractable. In this study, the temperature dependence of A is experimentally determined for a $Ni_2Mn_{0.8}In_{1.2}$ single crystal by measuring the 180° domain-wall width using off-axis electron holography and magnetocrystalline anisotropy. The theoretically expected power-law scaling with magnetization for A is shown to be applicable only in the low-temperature region (approximately half of the Curie temperature), and A starts to follow the power law with a significantly larger scaling exponent in the higher-temperature region. The decremental trends in the domain-wall width and the exchange length at elevated temperature seem to be attributed to this temperature dependence of A.

DOI: 10.1103/PhysRevB.101.014443

I. INTRODUCTION

The ferromagnetic exchange stiffness constant A and magnetocrystalline anisotropy constant K are indispensable information for spintronic and magnetically functional materials. As examples, they are the key parameters for tailoring multilayer spintronic devices [1] and for tuning the exchange length $l_{ex} \propto \sqrt{A/K}$ of magnetic materials [2]. Micromagnetic simulations also require them to simulate the dynamic evolution of spin configurations. Many micromagnetic platforms have dealt with the dynamics at low temperature, where the parameters of A and K of the materials do not show apparent temperature dependence. However, owing the increasing interest in thermally assisted magnetization dynamics, such as the spin-Seebeck effect [3], ultrafast laser-induced magnetization reversal [4], and magnetic skyrmion motion [5,6], a micromagnetic algorithm for the high-temperature dynamics has recently been developed [7–9]. A correct description of the temperature dependence of A and K has accordingly become a strong concern.

Whereas the temperature dependence of K can be determined unambiguously for the whole temperature range below the Curie temperature T_C as given later, that of A is nontrivial and confusing because there exist two different definitions of the so-called domain-wall (DW) stiffness and spin-wave (SW) stiffness, depending on the underlying interpretations with different length scale. In the analytically tractable case of DW stiffness, the following relation holds even at elevated temperatures:

$$\Delta F = 4\sqrt{AK}, \tag{1}$$

with the free energy ΔF of a domain wall. The ΔF has the form of $\Delta F(\beta) = \int_0^\beta \Delta E(\beta')d\beta'$, where ΔE is the energy difference between systems with and without a domain wall and $\beta = 1/k_BT$ (k_B: the Boltzmann constant) [10]. The ΔF and K in Eq. (1) show different temperature dependence, resulting in the nontrivial temperature dependence of A. On the other hand, the SW stiffness does not have a rigorous mathematical form and is evaluated from numerical simulations and spin-wave experiments. While the definitions of the DW stiffness and SW stiffness are independently derived, their magnitude and temperature dependence are predicted to be in good agreement [10].

The experimental consolidation of A has been still less practical because it generally requires significant efforts in, as examples, the fabrication of high-quality single crystals and performing highly specialized measurements such as spin-wave resonance measurements, inelastic neutron scattering, and Brillouin light scattering [11]. Considerable numerical scatter among the literature data, which arises from the quality of single-crystal and/or measurement methods, also makes the efforts less worthwhile [11–13]. The approximation $A \sim 1.0 \times 10^{-11}$ J/m is commonly recognized to hold for many soft magnets as the ground state [14] but is too imprecise to be applied at elevated temperatures. There is a limited number of experiments on the temperature dependence because of the requirement for temperature controllability and higher signal-to-noise ratio, especially near the T_C, while performing multiple measurements. However, theoretical studies on the magnetization dependence of A provide in-depth insights on this intractable problem: Atxitia *et al.* first predicted a quadratic scaling law with respect to the normalized spontaneous magnetization m, $A \propto m^2$ from a mean-field approximation [15], but later refined the scaling factor to be 1.715 for body-centered-cubic (bcc) ferromagnets under the different

*niitsu.koudai.8z@kyoto-u.ac.jp

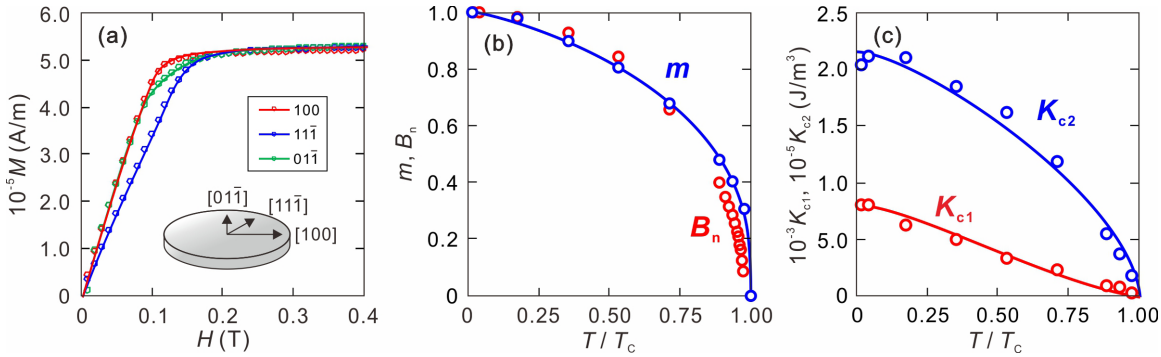

FIG. 1. (a) Relationship between magnetization (M) and magnetic field (H) at 4.2 K along [100], [11$\bar{1}$], and [01] directions. (b) Temperature dependences of normalized spontaneous magnetization m and normalized in-plane magnetic flux density B_n. The B_n can be derived from the electron holography observations. (c) Temperature dependences of magnetocrystalline anisotropy constants K_{c1} and K_{c2}.

spin models based on the domain-wall energy and the spin-wave dispersion wherein the correlation between different spin-wave modes is involved [10]. These predictions have been deduced to be valid at temperatures below $\sim T_C/4$.

Some authors have recently proposed an alternative method to explain the temperature dependence of the 180° domain-wall width δ observed in materials having a relatively small cubic magnetocrystalline anisotropy constant K_{c1} [16]. This suggests that the width of the 180° domain wall introduced in the thin-foiled specimen is dictated by the energy minimization, where the total energy γ_{total} is given as a summation of the exchange energy $\gamma_{ex} = A\pi^2/\delta$, the anisotropy energy $\gamma_{\text{ani}} = \delta K_{c1}/2$, and the magnetostatic energy $\gamma_{\text{mag}} = [\pi\delta^2/(\delta + D)]M_s^2$, that is, $\gamma_{\text{total}} = A\pi^2/\delta + \delta K_{c1}/2 + k[\pi\delta^2/(\delta + D)]M_s^2$ with a sample-dependent parameter k that modifies the significance of γ_{mag} relative to $\gamma_{ex} + \gamma_{\text{ani}}$. The energy minimization condition satisfies

$$\partial\gamma_{\text{total}}/\partial\delta = -A(\pi/\delta)^2 + K_{c1}/2 + \pi k M_s^2\delta(\delta + 2D)/(\delta + D)^2 = 0, \quad (2)$$

where D and M_s are the thickness of thin-foiled specimen and spontaneous magnetization, respectively. Equation (2) has successfully explained the temperature-insensitive δ variations observed in Fe and Ni thin foils, which is a completely different behavior from the well-known scalability of $\delta \propto \sqrt{A/K}$ in the bulk [17]. Because Eq. (2) allows us to evaluate A through microscopic magnetic imaging, such as Lorentz microscopy and electron holography, it will have an exclusive advantage for materials having difficulties in, as examples, the large-volume and/or high-purity fabrications.

A Ni-based Heusler alloy is a multiferroic material that exhibits a metamagnetic martensitic transformation [18] and hosts competing magnetism in relation to the change in the degree of atomic ordering: Ferromagnetic decoupling and antiferromagnetic coupling are promoted as the degree of atomic ordering decreases [19,20]. Indeed, it has been reported that antiferromagnetism arises at antiphase boundaries (APBs), where the degree of atomic ordering locally decays [21], thus the 180° domain walls preferentially locate at the APBs [22]. This has invoked interest in the temperature, chemical, and degree of atomic ordering dependences of the magnetic exchange length, which is a measure of the long-range magnetic interaction, because it may have an effect on the magnetic domain structure as well as the martensitic transformation behavior. In this study, the cubic magnetocrystalline anisotropy constants of K_{c1} and K_{c2} and A are examined for an off-stoichiometric $Ni_2Mn_{0.8}In_{1.2}$ Heusler alloy. This In-rich Heusler alloy does not undergo the metamagnetic martensitic transformation [23] but inherits potent antiferromagnetism in the disordered $B2$ structure, while ferromagnetism is robust in the ordered $L2_1$ Heusler structure.

II. EXPERIMENTAL METHOD

The ingot was fabricated by induction melting and subjected to homogenization at 1173 K for 12 h and subsequent annealing at 873 K for 4 d followed by quenching in ice water. Since the order/disorder ($L2_1/B2$) transition temperature was ~970 K [24], the obtained bulk had an $L2_1$ crystallinity with almost no thermal APBs. A (011)-oriented single-crystalline disk with ~2.5-mm diameter and ~0.7-mm thickness [see the inset schematic in Fig. 1(a)] was cut out from the bulk where the crystallographic orientation was checked by x-ray Laue diffraction. The orientation dependence of the magnetization curves was measured with respect to the [100], [11$\bar{1}$], and [01$\bar{1}$] directions at various temperatures below T_C using a superconducting quantum interference device. For the magnetic domain-wall observation, off-axis electron holography with double biprism interferometry [25] was employed using a 300-kV transmission electron microscope equipped with a well-calibrated liquid He cooling holder. A (100) thin-foiled specimen with 250 ± 10-nm thickness was lifted up using a focused ion beam. The detailed imaging and reconstructing processes were basically the same as the precedent work [16]. To improve the signal-to-noise ratio, more than ten reconstructed phase images were averaged into one at every settled temperature. The resultant spatial and phase resolutions were ~15.1 nm and ~0.10 rad, respectively. While the phase resolution was still not sufficient for this study, we have averaged over 270-nm width along the domain wall and have reduced the phase undulation to ~0.02 rad.

III. RESULTS AND DISCUSSION

The representative orientation dependence of magnetization curve is shown in Fig. 1(a). Similar to bcc-Fe, easy and hard axes of this alloy are the ⟨100⟩ and ⟨111⟩ directions,

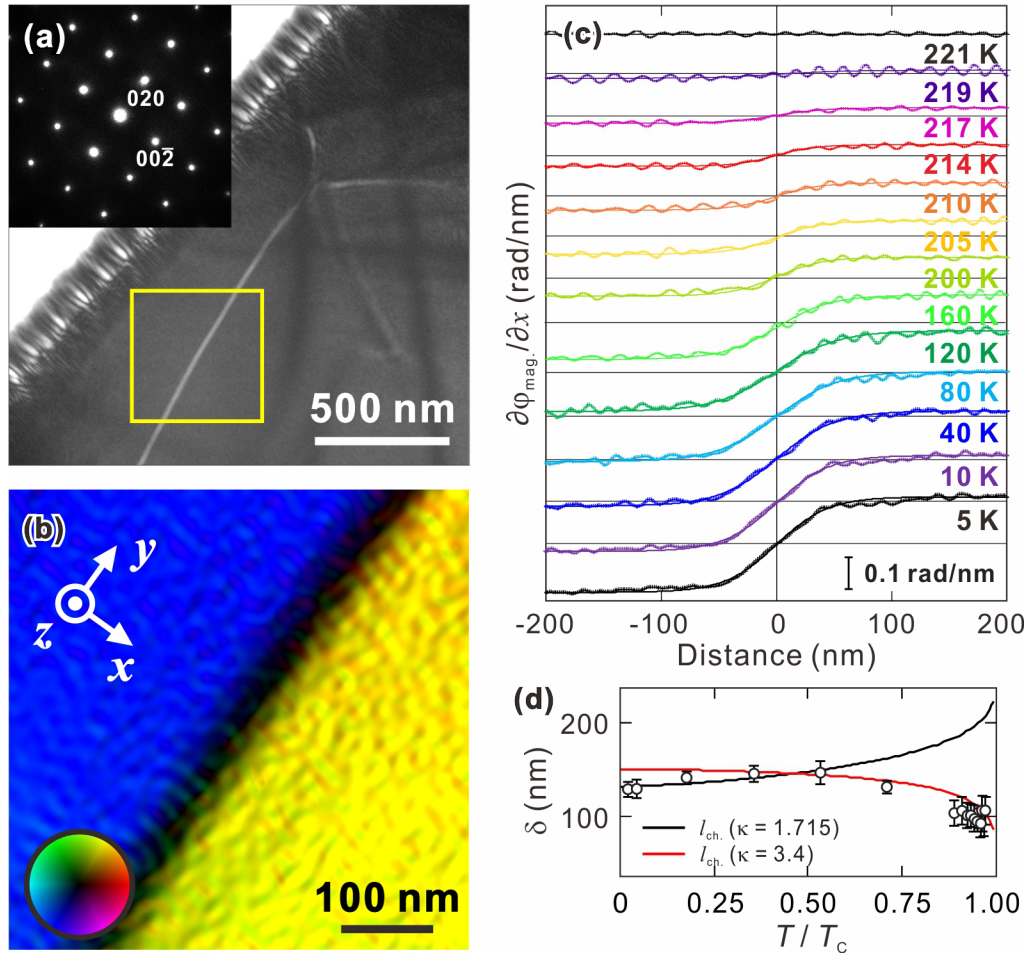

FIG. 2. (a) Lorentz image taken at 5 K (over focus). (b) Reconstructed magnetic phase (φ_{mag}) image of the region surrounded by the rectangle in (a). Color coding is assigned to the atan2(φ_{mag}) distribution, the absolute value and direction of which are identical to the brightness and color hue of the inserted color wheel. (c) Differential φ_{mag} profiles traversing the 180° domain wall at various settled temperatures. (d) Temperature dependence of domain-wall width δ.

respectively. The temperature dependence of M_s is derived from the *M-H* relationship and presented in the normalized form of m in Fig. 1(b). The inserted fitting curve is derived using the following equation proposed by Kuz'min:

$$m = [1 - s(T/T_C)^{3/2} - (1 - s)(T/T_C)^p]^{1/3}, \quad (3)$$

where s and p are fitting parameters [26]. A fitting curve with $p = 5/2$ and $s = 3/2$ can reproduce the experimental plots over the whole temperature range. The T_C and M_s at 0 K are determined to be 225 K and 5.4×10^5 A/m (5.4×10^2 emu/cm^3), respectively. Furthermore, K_{c1} and K_{c2} are approximated from Fig. 1(a), as shown in Fig. 1(c). The normalized magnetocrystalline anisotropy constants obey the power law (so-called Zener's theory [27]) with respect to m, that is,

$$K_{c1}/K_{c1}^\circ = m^{\alpha_1}, \quad K_{c2}/K_{c2}^\circ = m^{\alpha_2}, \quad (4)$$

where K_{c1}° and K_{c2}° are the magnetocrystalline anisotropy constants at 0 K. The fitting curves in Fig. 1(c) are derived with $\alpha_1 = 3.8$, $K_{c1}^\circ = 8.0 \times 10^3$ J/m^3, and $\alpha_2 = 1.7$, $K_{c2}^\circ = 2.1 \times 10^5$ J/m^3, where the temperature dependence of m is dictated by Eq. (3). Noteworthy is that K_{c2} is greater than K_{c1} by more than one order of magnitude at all examined temperatures. Meanwhile, an ideal Bloch-type 180° domain wall introduced in a (100) plane is assigned to a (010) or (001) in-plane rotation, which indicates that one of the directional cosines is always zero for this domain-wall geometry. The magnetocrystalline anisotropy energy E_a can be expanded as

$$E_a \simeq K_{c1}(\alpha_1^2\alpha_2^2 + \alpha_2^2\alpha_3^2 + \alpha_3^2\alpha_1^2) + K_{c2}\alpha_1^2\alpha_2^2\alpha_3^2, \quad (5)$$

with directional cosines α_1, α_2, and α_3. Considering the orientation of the domain wall, the contribution of the K_{c2} term becomes zero for an ideal Bloch-type 180° domain wall. Strictly speaking, complete Bloch-type rotation is not allowed and an asymmetric spin configuration is achieved owing to the contribution of γ_{mag}. Nevertheless, the numerical contribution of K_{c2} is considered to be still less significant, as demonstrated later, and Eq. (2) seems to be applicable for the observed 180° domain wall in the (100) thin foil of this material.

Figure 2(a) shows an over-focused Lorentz image taken at 5 K for the thin-foiled specimen. The white line running along nearly the [010] direction is identical to a 180° domain wall. Note that this wall remained stationary up to 219 K; this wall lay with almost no motion up to 219 K. Electron holography

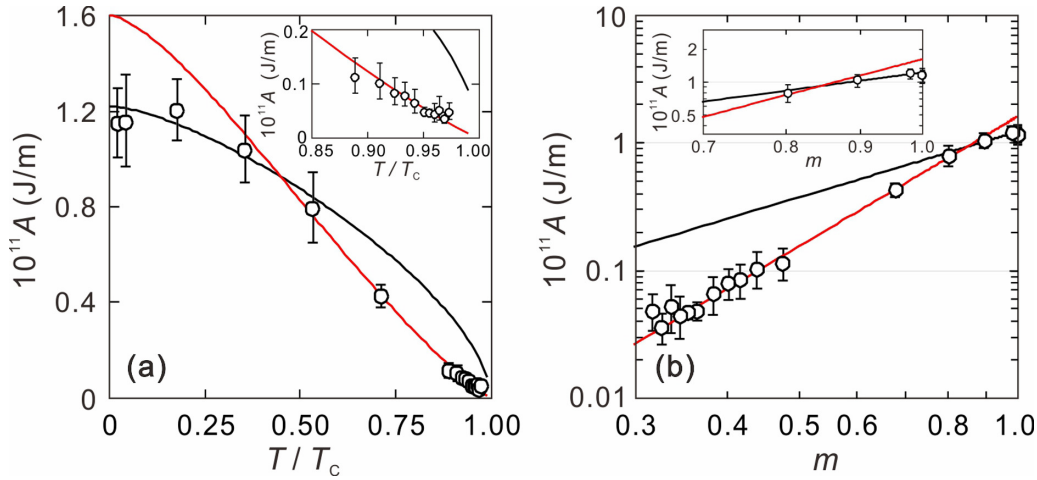

FIG. 3. Exchange stiffness constant A plotted as functions of (a) T/T_C and (b) m. The black and red lines are obtained with $\kappa = 1.715$ and 3.4, respectively.

observation was performed for the rectangle in Fig. 2(a): a representative reconstructed magnetic phase (φ_{mag}) image at 5 K is shown in Fig. 2(b). This image straightforwardly explains that the direction of the in-plane magnetic flux (B) is opposite across the domain wall. Regarding the spatial distribution of $\varphi_{mag.}$, we have

$$\frac{\partial \varphi_{mag}}{\partial x} = -\frac{e}{\hbar}\int B_y dz \simeq -\frac{e}{\hbar} B_y D, \tag{6}$$

where e, $\hbar$, and B_y represent the elementary charge, Dirac's constant, and the y component of B, respectively. [The x-y-z coordination is given in Fig. 2(b).] The latter approximation in Eq. (6) holds when B_y does not change along the z direction. From this equation, B_y at 5 K is determined to be 0.42 ± 0.02 T. The normalized magnetic flux B_n is plotted in Fig. 1(b) as a function of temperature. This shows good agreement with m, which indicated that this foil maintains the magnetic properties of the bulk. The $\partial\varphi_{mag}/\partial x$ variations across the domain wall at various settled temperatures are shown in Fig. 2(c). All profiles show high rotational symmetry with respect to the domain-wall center, which indicates the spin configuration is close to an ideal Bloch-type 180° rotation. This symmetric configuration is responsible for the small contribution of γ_{mag} to γ_{total} and thus we could propose that the Bloch-type picture with negligible effect of K_{c2} is applicable for this material. To derive the domain-wall width δ from this profile, the fitting curves with the function

$$\partial\varphi_{mag}/\partial x = I \tanh[\pi(x - x_{off})/\delta] \tag{7}$$

are also appended, where I and x_{off} are the amplitude and offset of distance x. Thereby we can calculate δ numerically as a function of the temperature, as shown in Fig. 2(d). Similar to that observed for a (100) Fe thin foil [16], δ does not exhibit an apparent sensitivity to the temperature change. This behavior clearly contradicts that of the well-known δ's scaling parameter of $\sqrt{A/K_{c1}}$, which shows a monotonous increase with increasing temperature [16]. A temperature-insensitive δ is mainly attributed to the presence of a surface, which pinches off domain walls to reduce the energy penalty of γ_{mag}.

Because the temperature dependences of K_{c1} and δ are obtained, we can derive the temperature dependence of A from Eq. (2). Note that k is set to 0.4: this value scales the exchange stiffness constant at 0 K, A°, but does not have an effect on the temperature function of A/A°. Taking into account the affinity between the derived A° of 1.2×10^{-11} J/m and the widely accepted approximation of $\sim 1.0 \times 10^{-11}$ J/m [14], as well as the comparability to $k = 0.5$ for a (100) Fe thin foil [16], $k = 0.4$ would be a reasonable approximation. Derived A values are plotted as functions of T/T_C [Fig. 3(a)] and m [Fig. 3(b)]. In both figures, the power-law relation $A/A^\circ = m^\kappa$ with $\kappa = 1.715$ [10] is given as the black lines. While the scaling with $\kappa = 1.715$ seems valid for the low-temperature region up to $\sim 0.4T_C$, it apparently fails to reproduce the experimental results at elevated temperatures. An alternative scaling with $\kappa = 3.4$, which provides the best fitting above $0.4T_C$, is presented as the red lines. The two scaling curves suggest that the temperature dependence of A may not be trivial and can roughly be classified into two temperature classes of $T \lesssim 0.4T_C$, where theoretical description is highly applicable, and $0.4T_C \lesssim T$, where the thermodynamic ensemble may not be sufficiently incorporated in theoretical studies. As another reason for this behavior of A, from an experimental implication, the possible correlation between A and γ_{mag} should be taken into further consideration: because the A component perpendicular to the foil plane is considered to be smaller than that within the foil plane, the increasing contribution of surfaces at elevated temperatures may result in an underestimation of the averaged A in the foil specimens. In-depth experiments for this possibility will be conducted in the near future.

The temperature dependence of δ with the different scaling exponents κ is provided in Fig. 2(d). The trend at elevated temperature is found to be totally different: while the curve with $\kappa = 1.715$ showed an accelerated increase similar to the temperature dependence of $\sqrt{A/K_{c1}}$, that with $\kappa = 3.4$ shows a gradual decrease which reproduces the experimental results at elevated temperatures.

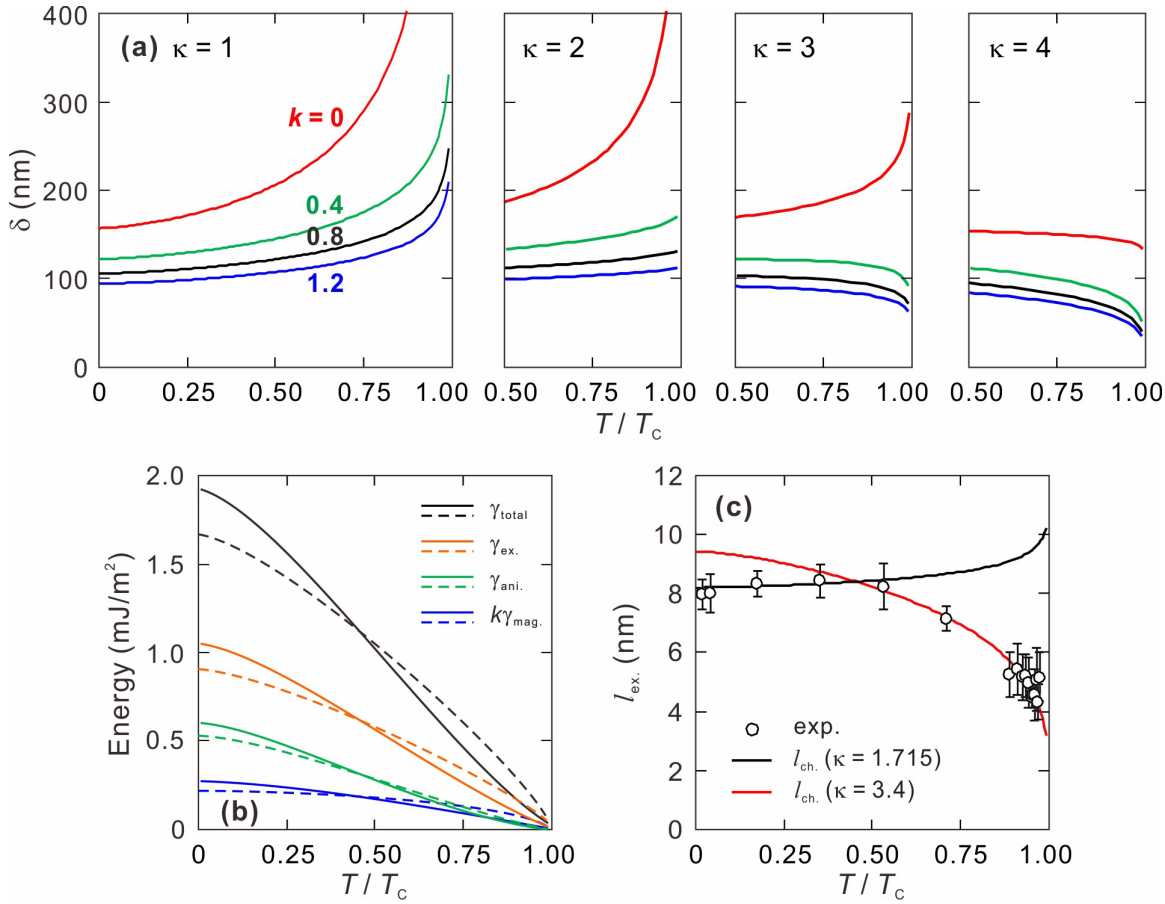

FIG. 4. (a) Temperature dependence of domain-wall width δ calculated with various sets of κ and k. (b) Energy breakdown as a function of T/T_C. The solid and dotted lines are obtained with $\kappa = 3.4$ and 1.715, respectively. (c) Exchange length l_{ex} as a function of T/T_C.

To evaluate the numerical significance of the parameters κ and k to δ, the temperature dependence of δ is presented in Fig. 4(a) for various sets of κ and k. As a general trend, an increase in k reduces the amplitude of the temperature dependency, but is not enough to reverse the trend when $\kappa \leqslant 2$, which fails to reproduce the experimental results. A larger κ seems to be more straightforward to explain the experimental results. The energy breakdown of the observed domain wall is given in Fig. 4(b) where the solid and dotted lines are obtained with $\kappa = 3.4$ and 1.715, respectively. All lines monotonously decrease and the relative significance of γ_{mag} becomes larger with increasing temperature, which is qualitatively similar to that observed for a (100) Fe thin foil [16]. The transition between the lines with $\kappa = 3.4$ and 1.715 is located at around $T \sim 0.4T_C$: a κ value giving a lower γ_{total} is favored. Finally, the exchange length $l_{ex} = \sqrt{A/2\pi M_s^2}$, which is the essential length scale for dictating magnetic reversal in magnets [14,28,29], is derived as shown in Fig. 4(c). Similar to the temperature dependence of δ, $l_{ex.}$ changes its trend from a slight increase to a significant decrease with increasing temperature. Again, this trend is not able to be explained with a single κ scaling.

IV. SUMMARY

In conclusion, we have examined the temperature dependence of A for an off-stoichiometric $Ni_2Mn_{0.8}In_{1.2}$ Heusler alloy using the measurements of magnetocrystalline anisotropy and of a 180° domain-wall width through electron holography observations. The power-law scaling $A/A^\circ \sim m^\kappa$ with $\kappa = 1.715$, which is given from the theoretical considerations, seems to be applicable below $0.4T_C$, but is supplanted by the scaling with a much larger κ of 3.4 above $0.4T_C$. The observed nontrivial temperature dependence of A, which has not been experimentally captured and not been theoretically predicted, results in the opposite temperature trends of δ and $l_{ex.}$. Toward the correct parametrization of A, the results highlight the fundamental but overlooked aspect of A and provide insights from an experimental approach on the effect of temperature.

ACKNOWLEDGMENTS

K.N. acknowledges financial support provided by a Grant-in-Aid for Young Scientists (B) (Grant No. 16K21632) from Japan Society for the Promotion of Science (JSPS) and Murata Science Foundation.

[1] E. B. Myers, D. C. Ralph, J. A. Katine, R. N. Louie, and R. A. Buhrman, Science **285**, 867 (1999).

[2] S. Okamoto, N. Kikuchi, O. Kitakami, T. Miyazaki, Y. Shimada, and K. Fukamichi, Phys. Rev. B **66**, 024413 (2002).

[3] K. Uchida, S. Takahashi, K. Harii, W. Koshibae, K. Ando, S. Maekawa, and E. Saitoh, Nature (London) **455**, 778 (2008).
[4] T. A. Ostler, J. Barker, R. F. L. Evans, R. W. Chantrell, U. Atxitia, O. Chubykalo-Fesenko, S. El Moussaoui, L. Le Guyader, E. Mengotti, L. J. Heyderman, F. Nolting, A. Tsukamoto, A. Itoh, D. Afanasiev, B. A. Ivanov, A. M. Kalashnikova, K. Vahaplar, J. Mentink, A. Kirilyuk, Th. Rasing, and A. V. Kimel, Nat. Commun. **3**, 666 (2012).
[5] L. Kong and J. Zang, Phys. Rev. Lett. **111**, 067203 (2013).
[6] M. Mochizuki, X. Z. Yu, S. Seki, N. Kanazawa, W. Koshibae, J. Zang, M. Mostovoy, Y. Tokura, and N. Nagaosa, Nat. Mater. **13**, 241 (2014).
[7] D. A. Garanin, Phys. Rev. B **55**, 3050 (1997).
[8] N. Kazantseva, D. Hinzke, U. Nowak, R. W. Chantrell, U. Atxitia, and O. Chubykalo-Fesenko, Phys. Rev. B **77**, 184428 (2008).
[9] R. F. L. Evans, D. Hinzke, U. Atxitia, U. Nowak, R. W. Chantrell, and O. Chubykalo-Fesenko, Phys. Rev. B **85**, 014433 (2012).
[10] U. Atxitia, D. Hinzke, O. Chubykalo-Fesenko, U. Nowak, H. Kachkachi, O. N. Mryasov, R. F. Evans, and R. W. Chantrell, Phys. Rev. B **82**, 134440 (2010).
[11] C. A. F. Vaz, J. A. C. Bland, and G. Lauhoff, Rep. Prog. Phys. **71**, 056501 (2008).
[12] T. Maeda, H. Yamauchi, and H. Watanabe, J. Phys. Soc. Jpn. **35**, 1635 (1973).
[13] E. P. Wohlfarth, *Ferromagnetic Materials Vol. 1*, edited by E. P. Wohlfarth (North-Holland, Amsterdam, 1980).
[14] G. S. Abo, Y.-K. Hong, J. Park, J. Lee, W. Lee, and B.-C. Choi, IEEE Trans. Magn. **49**, 4937 (2013).
[15] U. Atxitia, O. Chubykalo-Fesenko, U. Kazantseva, D. Hinzke, U. Nowak, and R. W. Chantrell, Appl. Phys. Lett. **91**, 232507 (2007).
[16] K. Niitsu, T. Tanigaki, K. Harada, and D. Shindo, Appl. Phys. Lett. **113**, 222407 (2018).
[17] A. Hubert and R. Schäfer, *Magnetic Domains* (Springer-Verlag, Berlin, 1998).
[18] R. Kainuma, Y. Imano, W. Ito, Y. Sutou, H. Morito, S. Okamoto, O. Kitakami, K. Oikawa, A. Fujita, T. Kanomata, and K. Ishida, Nature (London) **439**, 957 (2006).
[19] K. Yoshida, Phys. Rev. **106**, 893 (1957).
[20] D. P. Oxley, R. S. Tebble, and K. C. Williams, J. Appl. Phys. **34**, 1362 (1963).
[21] K. Niitsu, K. Minakuchi, X. Xu, M. Nagasako, I. Ohnuma, T. Tanigaki, Y. Murakami, D. Shindo, and R. Kainuma, Acta Mater. **122**, 166 (2017).
[22] A. J. Lapworth and J. P. Jakubovics, Philos. Mag. **29**, 253 (1974).
[23] Y. Sutou, Y. Imano, N. Koeda, T. Omori, R. Kainuma, K. Ishida, and K. Oikawa, Appl. Phys. Lett. **85**, 4358 (2004).
[24] T. Miyamoto, W. Ito, R. Y. Umetsu, R. Kainuma, T. Kanomata, and K. Ishida, Scr. Mater. **62**, 151 (2010).
[25] K. Harada, A. Tonomura, Y. Togawa, T. Akashi, and T. Matsuda, Appl. Phys. Lett. **84**, 3229 (2004).
[26] M. D. Kuz'min, Phys. Rev. Lett. **94**, 107204 (2005).
[27] C. Zener, Phys. Rev. **96**, 1335 (1954).
[28] W. F. Brown, Phys. Rev. **105**, 1479 (1957).
[29] E. H. Frei, S. Shtrikman, and D. Treves, Phys. Rev. **106**, 446 (1957).